

Supplementary Material

A - Summary of Experimental STEG Results

Author	Year	Efficiency	TE Material	γ_{op}	γ_{th}	T_h (°C)	T_c (°C)
Telkes [1]	1954	0.63%	ZnSb/BiSb (experimental)	1	1	80	35
Telkes [1]	1954	3.35%	ZnSb/BiSb (experimental)	50	1	260	20
Rush [2]	1964	0.7%	Bi ₂ Te ₃ (commercial)	-	-	-	-
Goldsmid [3]	1980	1.4%	Bi ₂ Te ₃ (commercial)	1	100	90	35
Goldsmid [3]	1980	0.5%	Bi ₂ Te ₃ (experimental)	3	-	150	30
Amatya & Ram [4]	2010	3%	Bi ₂ Te ₃ (commercial)	66	-	-	-
Suter [5]	2010	0.08%	Perovskite (experimental)	300	11	625	75
Kraemer [6]	2011	4.6%	Bi ₂ Te ₃ (exp, nanostructured)	1.5	200	200	20

TABLE I: A summary of experimental data from previous STEG studies.

B - Temperature Gradients Across the Absorber

Vertical Temperature Distribution

As discussed in the Methods section, the absorber surface temperature (T_{abs}) and the TE hot side temperature (T_h) will differ slightly. However, approximating these temperatures as equal makes for much simpler calculations. In order to justify this assumption, we have calculated the difference between T_{abs} and T_h as a function of T_h for several levels of incident flux. This calculation was performed for a 5 mm thick absorber with a κ_{abs} of 55 W/mK (an approximate value for graphite at 1000°C). The TE material has a κ_{TE} value of 1 W/mK and a constant zT of 1. We see that there is at most a 3.6% difference between T_{abs} and T_h .

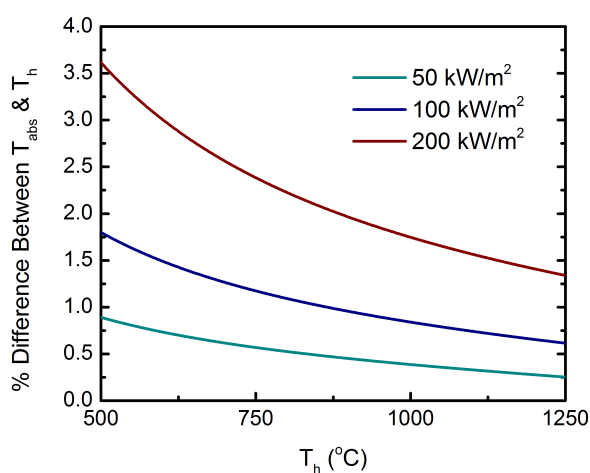


Fig. 1: Vertical temperature distribution across the absorber

Horizontal Temperature Distribution

The issue of temperature uniformity across the absorber has been addressed by Kraemer, et al. [6]. In this work the absorber is approximated as an annular fin, and the radial temperature distribution can be calculated using modified Bessel functions of the first and second order. Here, we assume that T_h is uniform across the TE leg, which has a diameter of 1 cm. We then plot the temperature difference over the entire absorber, which has a diameter of 5 cm (using the same absorber thickness and thermal conductivities as above). This 25-fold thermal concentration value is quite large for the thermal length values considered here.

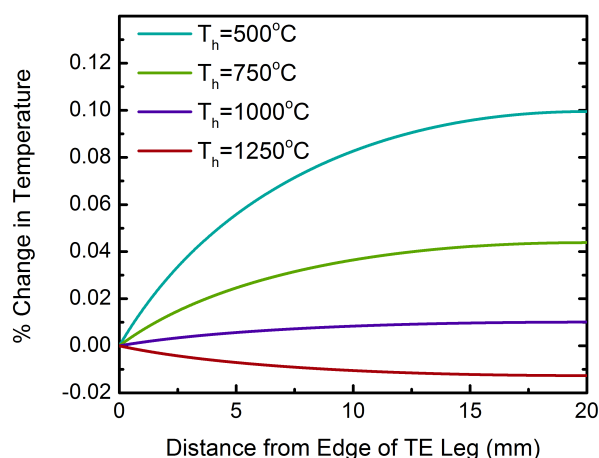


Fig. 2: Horizontal temperature distribution across the absorber

-
- [1] Telkes, M. Solar Thermoelectric Generators. *Journal of Applied Physics* **25**, 13 (1954).
- [2] Rush, R. E. Solar flat plate thermoelectric generator research (1964).
- [3] Goldsmid, H. J., Giutronich, J. E. & Kaila, M. M. Solar Thermoelectric Generation Using Bismuth Telluride Alloys. *Solar Energy* **24**, 435–440 (1980).
- [4] Amatya, R. & Ram, R. J. Solar Thermoelectric Generator for Micropower Applications. *Journal of Electronic Materials* **39**, 1735–1740 (2010).
- [5] Suter, C., Tomes, P., Weidenkaff, A. & Steinfeld, A. Heat Transfer and Geometrical Analysis of Thermoelectric Converters Driven by Concentrated Solar Radiation. *Materials* **3**, 2735–2752 (2010).
- [6] Kraemer, D. *et al.* High-performance flat-panel solar thermoelectric generators with high thermal concentration. *Nature Materials* **10**, 532–538 (2011).